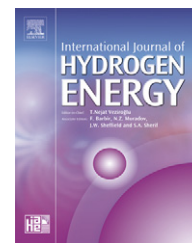


Available at [www.sciencedirect.com](http://www.sciencedirect.com)journal homepage: [www.elsevier.com/locate/ijhe](http://www.elsevier.com/locate/ijhe)

## Technical Communication

# Two-phase transport in the cathode gas diffusion layer of PEM fuel cell with a gradient in porosity

Falin Chen<sup>a</sup>, Min-Hsing Chang<sup>b,\*</sup>, Ping-Tso Hsieh<sup>a</sup>

<sup>a</sup>Institute of Applied Mechanics, National Taiwan University, Taipei 107, Taiwan, ROC

<sup>b</sup>Department of Mechanical Engineering, Tatung University, Taipei 104, Taiwan, ROC

### ARTICLE INFO

#### Article history:

Received 29 February 2008

Accepted 29 February 2008

Available online 16 April 2008

#### Keywords:

PEM fuel cell

Cathode gas diffusion layer

Porosity gradient

Two-phase transport

### ABSTRACT

Two-phase transport in the cathode gas diffusion layer (GDL) of a proton exchange membrane fuel cell (PEMFC) is studied with a porosity gradient in the GDL. The porosity gradient is formed by adding micro-porous layers (MPL) with different carbon loadings on the catalyst layer side and on the flow field side. The multiphase mixture model is employed and a direct numerical procedure is used to analyze the profiles of liquid water saturation and oxygen concentration across the GDL as well as the resulting activation and concentration losses. The results show that a gradient in porosity will benefit the removal rate of liquid water and also enhance the transport of oxygen through the cathode GDL. The present study provides a theoretical support for the suggestion that a GDL with porosity gradient will improve the cell performance.

© 2008 International Association for Hydrogen Energy. Published by Elsevier Ltd. All rights reserved.

## 1. Introduction

The proton exchange membrane fuel cell (PEMFC) has widely promising applications in many power systems. However, due to its low operating temperature generally under 90 °C, the water vapor produced in cathode side may condense and cause the so-called ‘flooding’ phenomena. The condensation of water vapor will block the pores of gas diffusion layer (GDL) and then result in the reduction of oxygen transport to the catalyst layer. Therefore, the water management is quite important in the cathode side to avoid the accumulation of liquid water and thus enhance the oxygen transport for the improvement of cell performance. Accordingly, it is considerable to understand the two-phase transport characteristics in the cathode GDL and the effective ways to remove excessive water.

Numerous studies have devoted to investigating the two-phase flow and transport in the cathode of PEMFC [1–15]. Particularly, a novel design of GDL in which contains a micro-porous layer (MPL) has been proposed to provide better gas and water transport performance [10–15]. The MPL is composed of carbon black power and hydrophobic agent such as PTFE and then applied on one side or two sides of the GDL. The addition of MPL has been found to give a more proper pore structure and wettability to obtain effective gas and water transport. Moreover, it also helps to decrease the electric contact resistance between the GDL and the adjacent catalyst layer or flow plate. Pasaogullari and Wang [10] first developed a one-dimensional model based on the multiphase mixture formulation to investigate the effect of the MPL on two-phase transport across the cathode GDL. They further consider a full cell model and analyze the two-phase

\*Corresponding author. Tel.: +886 2 25925252x3410 512; fax: +886 2 25997142.

E-mail addresses: [mhchang@ttu.edu.tw](mailto:mhchang@ttu.edu.tw), [mhchang@so-net.net.tw](mailto:mhchang@so-net.net.tw) (M.-H. Chang).

transport in PEMFCs with bilayer cathode GDL, which consists of a coarse GDL and a MPL. They examined the effects of porosity, thickness and wettability of the MPL and found that the back-flow of liquid water increases with increasing hydrophobicity and thickness, and decreasing porosity of the MPL [11]. Weber and Newman [12] also developed a theoretical model to study the effects of MPL and found that the use of MPL is beneficial to keep water out of the cathode GDL and move it through the anode. Wang et al. [13] focused on the effects of carbon black in MPL and extensively examined the physical properties of GDL including surface morphology, gas permeability, hydrophobic character, porosity and conductivity. They further prepared MPLs with different carbon materials and proposed that a novel GDL with a gradient in porosity formed by coating MPLs with different carbon loadings on the catalyst layer side and on the flow field side will improve the removal of liquid water [14]. Tang et al. [15] investigated the effect of porosity-graded MPL and obtained a better cell performance for a PEMFC with a porosity-graded MPL. They suggested that it is probably due to the facilitation of liquid water transport through large pores and gas diffusion via small pores.

Since the related experimental evidences [13–15] showed that a gradient in porosity of GDL will enhance the transport of gas reactant and the removal of liquid water in the cathode of PEMFC. Accordingly, a two-phase flow model for the cathode of PEMFC with a porosity gradient in GDL will be developed in this study. In addition, the effects of transport characteristics on the cell performance also will be examined. The simulating results provide a theoretical understanding for the influences of porosity gradient in GDL on the performance of PEMFC.

## 2. Theoretical model

The system configuration is shown in Fig. 1 for the GDL in the cathode side of a PEMFC with thickness  $L$ . The oxygen flux enters the GDL at the interface  $x=0$  and then diffuses through the GDL to the catalyst layer. The catalyst layer is assumed to be infinitely thin and locates at the interface  $x=L$  where the electrochemical reaction occurs. The pore size near the interface  $x=0$  is assumed to be larger than that on the other side  $x=L$  and thus a porosity

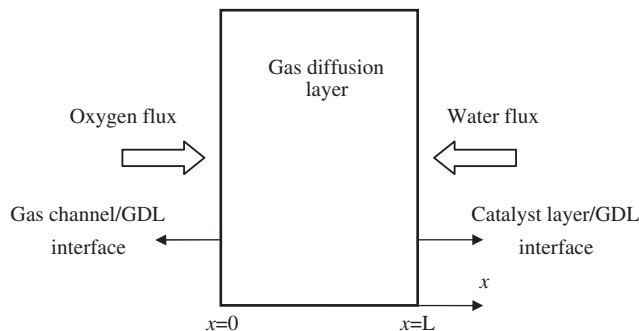


Fig. 1 – The configuration of simulation domain.

gradient exists in the GDL. In order to simplify the development of theoretical model, the system is supposed to be isothermal and under steady state condition. The gas phase is treated as an ideal gas and insoluble in the liquid phase. Based on the multiphase mixture model for the two-phase transport in the GDL, the continuity equation can be expressed by

$$\nabla \cdot (\rho \mathbf{u}) = 0, \quad (1)$$

where  $\rho$  is the two-phase mixture density and  $\mathbf{u}$  is the superficial two-phase mixture velocity. The species conservation equation can be written as

$$\begin{aligned} \nabla \cdot [\varepsilon(x)\gamma_\alpha \rho \mathbf{u} C^\alpha] &= \nabla \cdot [\varepsilon(x)\rho D^\alpha \nabla C^\alpha] + \nabla \cdot \{ \varepsilon(x) \\ &\times [\rho_l s D_l^\alpha \nabla C_l^\alpha + \rho_g (1-s) D_g^\alpha \nabla C_g^\alpha \\ &- \rho D^\alpha \nabla C^\alpha] \} - \nabla \cdot [(C_l^\alpha - C_g^\alpha) \mathbf{j}_1], \end{aligned} \quad (2)$$

where the superscript  $\alpha$  denotes the species and the subscripts l and g denote the liquid and gas phases, respectively. The notation  $C$  is the concentration,  $D$  the diffusion coefficient,  $\gamma$  the advection correction factor,  $s$  the saturation of liquid water,  $\mathbf{j}$  the diffusive mass flux and  $\varepsilon$  the porosity which is a function of position in the form

$$\varepsilon(x) = \varepsilon_1 + (\varepsilon_2 - \varepsilon_1) \frac{x}{L}, \quad (3)$$

where  $\varepsilon_1$  and  $\varepsilon_2$  are, respectively, the porosities at the interfaces  $x=0$  and  $L$ . The liquid water saturation  $s$  represents the ratio of the liquid water volume to the void pore volume. The quantities of the mixture in Eq. (2) and the definition of  $\gamma$  could be found in many related studies (cf. [9–11]) and thus will not be repeated here. The mass flux of liquid phase  $\mathbf{j}_1$  is given by

$$\mathbf{j}_1 = \frac{K \lambda_l \lambda_g}{\nu} \nabla P_c, \quad (4)$$

where  $K$  is the permeability,  $\lambda$  the mobility,  $P_c$  the capillary pressure and  $\nu$  the mixture kinematic viscosity. The capillary pressure between the gas and liquid phases is related to the liquid water saturation in the form [2]

$$P_c = \sigma \cos(\theta_c) \left[ \frac{\varepsilon(x)}{K} \right]^{1/2} J(s), \quad (5)$$

where  $\sigma$  is the surface tension of liquid water,  $\theta_c$  the contact angle and  $J(s)$  the Leverett function [8]. Here a hydrophobic GDL ( $90^\circ < \theta_c < 180^\circ$ ) is considered and accordingly the function  $J(s)$  is given by

$$J(s) = 1.417s - 2.12s^2 + 1.263s^3. \quad (6)$$

Substituting Eq. (5) in Eq. (4), the mass flux  $\mathbf{j}_1$  can then be expressed by

$$\mathbf{j}_1 = \frac{K \lambda_l \lambda_g}{\nu} \sigma \cos(\theta_c) \left[ \frac{\varepsilon(x)}{K} \right]^{1/2} \frac{dJ(s)}{ds} \frac{ds}{dx}. \quad (7)$$

It is noted that the concentration of water vapor in the mixture  $C_g^{H_2O}$  can be written as

$$C_g^{H_2O} = \frac{\rho_v^{H_2O}}{\rho_g} = \frac{P_v M^{H_2O}}{P M^{air}}, \quad (8)$$

where  $M$  is the molecular weight and the concentration of liquid water  $C_l^{H_2O}$  is defined as

$$C_l^{H_2O} = 1. \quad (9)$$

When the GDL is saturated with water vapor, the concentration of water vapor is assumed to be uniform and thus the gas phase diffusion vanishes. Therefore, the species conservation equation (2) can be reduced to the following form:

$$\nabla \cdot [\varepsilon(x)\gamma_{\text{H}_2\text{O}}\rho\mathbf{u}C^{\text{H}_2\text{O}}] + \nabla \cdot \left[ \left( 1 - \frac{\rho_{\text{v}}^{\text{H}_2\text{O}}}{\rho_{\text{g}}} \right) \mathbf{j}_1 \right] = 0. \quad (10)$$

The continuity equation (1) also can be integrated over the GDL [10] to obtain

$$\rho\mathbf{u} = -\frac{I}{2F}(1+2\alpha)M^{\text{H}_2\text{O}} + \frac{I}{4F}M^{\text{O}_2}, \quad (11)$$

where  $I$  is the current density,  $F$  the Faraday constant and  $\alpha$  the net water transport coefficient from the anode to the cathode in the cell. The terms in the right-hand side of Eq. (11) is caused by the electrochemical reactions which occur on the interface of catalyst layer. By combining Eqs. (7)–(11) and then integrating the resultant equation over the GDL, the governing equation for water transport can be derived and written by

$$\begin{aligned} \varepsilon(x) \left( \lambda_1 + \lambda_g \frac{\rho_{\text{v}}^{\text{H}_2\text{O}}}{\rho_{\text{g}}} \right) \left[ -\frac{I}{2F}(1+2\alpha)M^{\text{H}_2\text{O}} + \frac{I}{4F}M^{\text{O}_2} \right] \\ + \left( 1 - \frac{\rho_{\text{v}}^{\text{H}_2\text{O}}}{\rho_{\text{g}}} \right) \frac{K\lambda_1\lambda_g}{v} \sigma \cos(\theta_c) \left[ \frac{\varepsilon(x)}{K} \right]^{1/2} \frac{dJ(s)}{ds} \frac{ds}{dx} \\ = -\frac{I}{2F}M^{\text{H}_2\text{O}}(1+2\alpha). \end{aligned} \quad (12)$$

For the oxygen transport, since oxygen is assumed to be insoluble in the liquid phase, the concentration  $C_1^{\text{O}_2}$  is equal to zero. Consequently, the conservation equation (2) for the species of oxygen becomes

$$\nabla \cdot [\varepsilon(x)\gamma_{\text{O}_2}\rho\mathbf{u}C^{\text{O}_2}] = \nabla \cdot [\varepsilon(x)\rho_{\text{g}}(1-s)D_{\text{g}}^{\text{O}_2}\nabla C_{\text{g}}^{\text{O}_2}] + \nabla \cdot (C_{\text{g}}^{\text{O}_2}\mathbf{j}_1), \quad (13)$$

Substituting Eqs. (7) and (11) in Eq. (13) and similarly integrating the resultant equation over the GDL, we can obtain the governing equation for the oxygen transport in the form

$$\begin{aligned} \lambda_g C_{\text{g}}^{\text{O}_2} \left[ -\frac{I}{2F}(1+2\alpha)M^{\text{H}_2\text{O}} + \frac{I}{4F}M^{\text{O}_2} \right] \\ - \left[ C_{\text{g}}^{\text{O}_2} \frac{K\lambda_1\lambda_g}{v} \sigma \cos(\theta_c) \left[ \frac{\varepsilon(x)}{K} \right]^{1/2} \frac{dJ(s)}{ds} \frac{ds}{dx} \right] \\ - \left[ \varepsilon(x)\rho_{\text{g}}(1-s)D_{\text{g}}^{\text{O}_2,\text{eff}} \frac{dC_{\text{g}}^{\text{O}_2}}{dx} \right] = \frac{I}{4F}M^{\text{O}_2}, \end{aligned} \quad (14)$$

where  $D_{\text{g}}^{\text{O}_2,\text{eff}}$  is the effective diffusion coefficient of oxygen modified by the Bruggeman correlation with tortuosity factor 1.5 as given in the equation below:

$$D_{\text{g}}^{\text{O}_2,\text{eff}} = [\varepsilon(1-s)]^{1.5} D_{\text{g}}^{\text{O}_2}. \quad (15)$$

To solve Eqs. (12) and (14), two boundary conditions have to be given. One of them is the assumption that the interface at  $x=0$  is free from liquid water and thus the liquid water saturation  $s$  should be zero there. Accordingly, we have

$$s = 0 \quad \text{at } x = 0. \quad (16)$$

The other boundary condition for the oxygen concentration can be derived from the convective mass transport analysis for the gas channel by employing the heat and mass transfer

**Table 1 – Parameters used in simulations**

Temperature, $T$ (K)	353
Air pressure, $P_c$ (Pa)	$1.013 \times 10^5$
Universal gas constant $R$ (J mol <sup>-1</sup> K <sup>-1</sup> )	8.314
Faraday constant, $F$	96487
Oxygen diffusion coefficient, $D_{\text{g}}^{\text{O}_2}$ (m <sup>2</sup> s <sup>-1</sup> )	$1.805 \times 10^{-5}$
Oxygen fraction, $C_{\text{g},\text{in}}^{\text{O}_2}$	0.21
Net water transport coefficient, $\alpha$	0.5
Gas diffusion layer thickness, $L$ (m)	$3 \times 10^{-4}$
Liquid water kinematic viscosity, $\nu_l$ (m <sup>2</sup> s <sup>-1</sup> )	$3.65 \times 10^{-7}$
Air kinematic viscosity, $\nu_g$ (m <sup>2</sup> s <sup>-1</sup> )	$2.07 \times 10^{-5}$
Surface tension, $\sigma$ (Nm <sup>-1</sup> )	0.0625
Charge transfer coefficient, $\alpha_c$	1.0

analogy [10]. Thus, the oxygen concentration  $C_{\text{g}}^{\text{O}_2}$  at the interface  $x=0$  is determined by

$$C_{\text{g}}^{\text{O}_2} \Big|_{x=0} = C_{\text{g},\text{in}}^{\text{O}_2} - \frac{M^{\text{O}_2} I}{4h_m \rho_{\text{g}}^{\text{air}} F}, \quad (17)$$

where  $C_{\text{g},\text{in}}^{\text{O}_2}$  is the oxygen concentration at the inlet of gas channel and  $h_m$  is the convective mass transfer coefficient. Eqs. (12) and (14) together with the boundary conditions (16) and (17) are solved by a fourth-order Runge–Kutta method with adaptive step size technique. Note that the electrochemical reaction at the interface of catalyst layer can be characterized by the Butler–Volmer equation below:

$$I = (1-s)I_{\text{ref}} \frac{C_{\text{g}}^{\text{O}_2} \Big|_{x=L}}{C_{\text{g},\text{ref}}^{\text{O}_2}} \exp\left(\frac{\alpha_c F}{RT} \eta\right), \quad (18)$$

where  $I_{\text{ref}}$  is the exchange current density at the reference oxygen concentration  $C_{\text{g},\text{ref}}^{\text{O}_2}$ ,  $\alpha_c$  the cathode charge transfer coefficient,  $F$  the Faraday constant,  $R$  the universal gas constant,  $T$  the absolute temperature and  $\eta$  the overpotential. The modification term  $(1-s)$  is used to account for the reduction of active surface due to liquid water coverage of catalyst particles. The overpotential estimated from Eq. (18) contains both activation and concentration losses and the cell potential excluding the ohmic losses can be determined by

$$V = V_{\text{oc}} - \eta, \quad (19)$$

where  $V_{\text{oc}}$  is the open circuit voltage. Since the proton conducting membrane is not considered in the present model, the ohmic losses caused mainly by the membrane will not be discussed here. The parameters used in the calculations are given in Table 1.

### 3. Results and discussions

We first show the liquid water saturation and oxygen concentration profiles across the GDL for a typical operating condition and then discuss the variations of polarization curves. Four typical cases are considered in which the porosity  $\varepsilon_2$  at the GDL/catalyst layer interface is fixed at 0.2 and the porosities  $\varepsilon_1$  at the GDL/gas channel interface

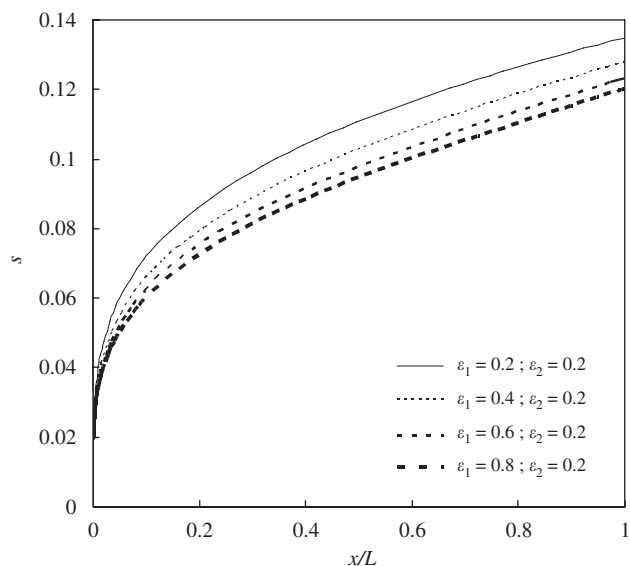


**Fig. 2 – Profiles of liquid water saturation across the GDL for four typical cases of porosity gradient.**

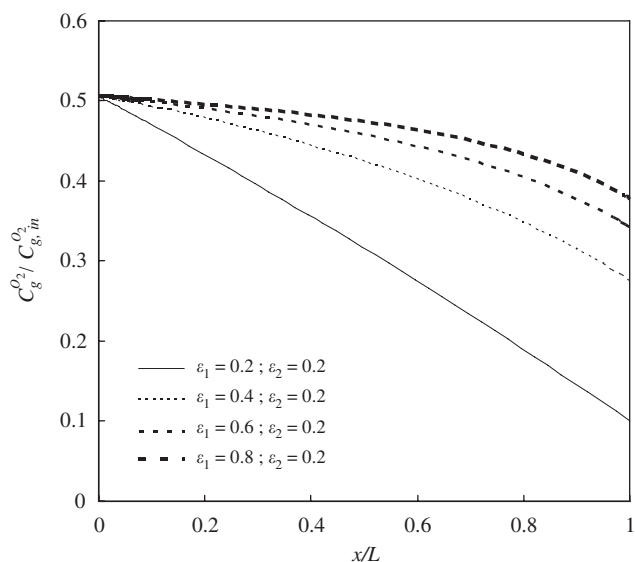


**Fig. 3 – Profiles of oxygen concentration across the GDL for four typical cases of porosity gradient.**

are 0.2, 0.4, 0.6 and 0.8, respectively. The cell operates at current density  $I = 1.2 \text{ A cm}^{-2}$  is chosen as the typical case and the corresponding liquid water saturation and oxygen concentration profiles are demonstrated, respectively, in Figs. 2 and 3 for the four cases with different gradients in porosity. As shown in Fig. 2, the liquid water saturation in the GDL indeed will decrease gradually with an increase of porosity gradient. This result theoretically confirmed that the coating of carbon power on one side of GDL to generate a gradient in porosity will be helpful for the removal of liquid water within the cathode GDL. This effect will become more pronounced when the operating condition gradually closes to the limiting current density state. The

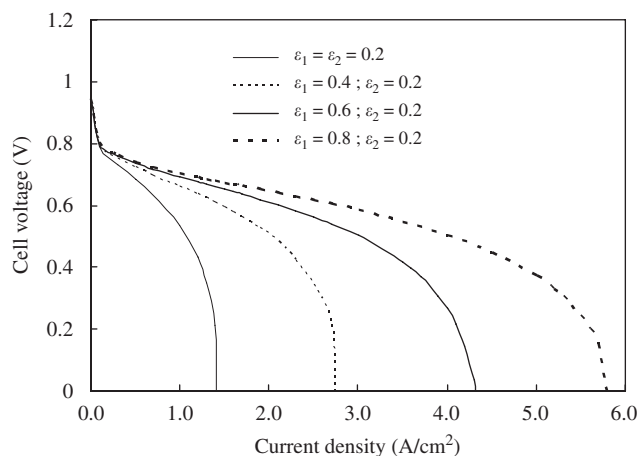


**Fig. 4 – I-V curves for four typical cases of porosity gradient.**

results illustrated in Fig. 3 also show that the transport of oxygen can be enhanced with porosity-gradient structure in the GDL. For the case of constant porosity  $\varepsilon_1 = \varepsilon_2 = 0.2$ , the concentration of oxygen simply decreases linearly across the GDL thickness which has been found in related studies [9,10]. However, the existence of porosity gradient can lower the transport resistance and thus the oxygen concentration descends more slowly from the gas channel side to the catalyst layer. This effect is more significant for a larger porosity gradient and results in a higher mean oxygen concentration within the GDL, and also raise the oxygen concentration reaching to the catalyst layer. Accordingly, the overpotential contributed from the concentration losses could be reduced and thus we could obtain a higher output of cell voltage. These results indicate the cell performance could be improved efficiently by the utilization of GDL with porosity gradient in the cathode side. The corresponding polarization curves are demonstrated in Fig. 4. Obviously, the limiting current density which is primarily dominated by the concentration losses will increase greatly by an increase of porosity gradient in GDL. Note that the ohmic losses are not considered here. In general, a higher porosity at interface  $x = 0$  also implies a higher contact resistance at the gas channel/GDL interface due to the worse electrical contact properties. Therefore, this factor should be taken into consideration in practical applications of GDL. A double-side coating of carbon power could be a possible solution [14] and some commercial products of GDL with double-side coating have already been available. The effects of permeability and contact angle together with porosity gradient also can be examined by the present model. In the general GDLs without porosity gradient, it has been found that a higher permeability and an increase of contact angle will improve the cell performance [9,10]. When the effect of porosity gradient is added, it is found that the two-phase transport and cell performance can be enhanced further. The corresponding results are similar to the typical case considered in Figs. 2–4, which suggest that a porosity-graded GDL with high permeability and contact angle will be the most efficient way to improve the properties of GDL.

---

#### 4. Conclusions

In this study, we have developed a two-phase flow model based on the multiphase mixture concept to investigate the transport characteristics in the cathode GDL of a PEMFC with a gradient in porosity. The results are consistent with experimental findings and provide a theoretical support to confirm that a porosity-graded structure in the GDL indeed can enhance the two-phase transport performance. The removal of liquid water within the GDL will be improved and the oxygen concentration approaching the catalyst layer will be increased. Consequently, the concentration losses will reduce significantly and results in a better cell performance. Further studies which focus on the two-layer GDL with a porosity gradient in each layer will be valuable to be explored in future.

---

#### Acknowledgments

The financial supports for this research from National Science Council of Taiwan through the grant NSC 95-2212-E-036-051

and Tatung University through the grant B96-M04-039 are gratefully acknowledged.

---

#### REFERENCES

- [1] Wang CY, Cheng P. *Int J Heat Mass Transfer* 1996;39:3607–18.
- [2] Wang CY, Cheng P. *Adv Heat Transfer* 1997;30:93–196.
- [3] He W, Yi JS, Nguyen TV. *AIChE J* 2000;46:2053–64.
- [4] Wang ZH, Wang CY, Chen KS. *J Power Sources* 2001;94:40–50.
- [5] Natarajan D, Nguyen TV. *J Electrochem Soc* 2001;148:1324–35.
- [6] You L, Liu H. *Int J Heat Mass Transfer* 2002;45:2277–87.
- [7] Berning T, Djilali N. *J Electrochem Soc* 2003;150:1589–98.
- [8] Pasaogullari U, Wang CY. *J Electrochem Soc* 2004;151:399–406.
- [9] Chang MH, Chen F, Teng HS. *J Power Sources* 2006;160:268–76.
- [10] Pasaogullari U, Wang CY. *Electrochim Acta* 2004;49:4359–69.
- [11] Pasaogullari U, Wang CY, Chen KS. *J Electrochem Soc* 2005;152:A1574–82.
- [12] Weber AZ, Newman J. *J Electrochem Soc* 2005;152:A677–88.
- [13] Wang XL, Zhang HM, Zhang JL, Xu HF, Tian ZQ, Chen J, et al. *Electrochim Acta* 2006;51:4909–15.
- [14] Wang X, Zhang H, Zhang J, Xu H, Zhu X, Chen J, et al. *J Power Sources* 2006;162:474–9.
- [15] Tang H, Wang S, Pan M, Yuan R. *J Power Sources* 2007;166:41–6.